

Thermodynamic and dynamic anomalies for a three-dimensional isotropic core-softened potential

Cite as: J. Chem. Phys. **124**, 084505 (2006); <https://doi.org/10.1063/1.2168458>

Submitted: 10 November 2005 . Accepted: 29 December 2005 . Published Online: 23 February 2006

Alan Barros de Oliveira, Paulo A. Netz, Thiago Colla, and Marcia C. Barbosa



View Online



Export Citation

ARTICLES YOU MAY BE INTERESTED IN

[Structural anomalies for a three dimensional isotropic core-softened potential](#)

The Journal of Chemical Physics **125**, 124503 (2006); <https://doi.org/10.1063/1.2357119>

[Comparison of simple potential functions for simulating liquid water](#)

The Journal of Chemical Physics **79**, 926 (1983); <https://doi.org/10.1063/1.445869>

[Core-softened potentials and the anomalous properties of water](#)

The Journal of Chemical Physics **111**, 8980 (1999); <https://doi.org/10.1063/1.480241>





Lock-in Amplifiers

Zurich Instruments

Watch the Video

Thermodynamic and dynamic anomalies for a three-dimensional isotropic core-softened potential

Alan Barros de Oliveira^{a)}

Universidade Federal do Rio Grande do Sul, Caixa Postal 15051, 91501-970, Porto Alegre, Rio Grande do Sul, Brazil

Paulo A. Netz

Departamento de Química, ULBRA, Canoas, Rio Grande do Sul, Brazil and Departamento de Química, Unilasalle, Canoas, Rio Grande do Sul, Brazil

Thiago Colla and Marcia C. Barbosa

Universidade Federal do Rio Grande do Sul, Caixa Postal 15051, 91501-970, Porto Alegre, Rio Grande do Sul, Brazil

(Received 10 November 2005; accepted 29 December 2005; published online 23 February 2006)

Using molecular-dynamics simulations and integral equations (Rogers-Young, Percus-Yevick, and hypernetted chain closures) we investigate the thermodynamics of particles interacting with continuous core-softened intermolecular potential. Dynamic properties are also analyzed by the simulations. We show that, for a chosen shape of the potential, the density, at constant pressure, has a maximum for a certain temperature. The line of temperatures of maximum density (TMD) was determined in the pressure-temperature phase diagram. Similarly the diffusion constant at a constant temperature, D , has a maximum at a density ρ_{\max} and a minimum at a density $\rho_{\min} < \rho_{\max}$. In the pressure-temperature phase diagram the line of extrema in diffusivity is outside of the TMD line. Although this interparticle potential lacks directionality, this is the same behavior observed in simple point charge/extended water. © 2006 American Institute of Physics. [DOI: [10.1063/1.2168458](https://doi.org/10.1063/1.2168458)]

I. INTRODUCTION

Water is an anomalous substance in many respects. Most liquids contract upon cooling. This is not the case of water, a liquid where the specific volume at ambient pressure starts to increase when cooled below $T=4\text{ }^{\circ}\text{C}$.¹ Besides, in a certain range of pressures, it also exhibits an anomalous increase of compressibility and specific heat upon cooling.²⁻⁴ Far less known are its dynamics anomalies: while for most materials diffusivity decreases with increasing pressure, liquid water has an opposite behavior in a large region of the phase diagram.⁵⁻¹³ The increase of diffusivity of water as the pressure is increased is related to the competition between the local ordered tetrahedral structure of the first neighbors and the distortions of the structure of the first and second neighbors. In the region of the phase diagram where this ordered structure is dominant, increasing pressure implies breaking first neighbor hydrogen bonds which allow for interstitial second neighbors to be in a closer approach. The interactions are thus weakened and therefore, although the system is more dense it has a larger mobility. In this sense, a good model for water and tetrahedral liquids should not only exhibit thermodynamic but also dynamic anomalies. In simple point charge/extended (SPC/E) water, the region of the pressure-temperature (p - T) phase diagram where the density anomaly appears is contained within the region of the p - T

phase diagram where anomalies in the diffusivity are present.^{9,10}

For explaining the thermodynamic anomalies, it was proposed that these anomalies are related to a second critical point between two liquid phases, a low-density liquid (LDL) and a high-density liquid¹⁴ (HDL) located at the supercooled region beyond the line of homogeneous nucleation and thus it cannot be experimentally measured.

Water, however, is not an isolated case. There are also other examples of tetrahedrally bonded molecular liquids such as phosphorus^{15,16} and amorphous silica¹⁷ that are also good candidates for having two liquid phases. Moreover, other materials such as liquid metals¹⁸ and graphite¹⁹ also exhibit thermodynamic anomalies. Unfortunately a coherent and general interpretation of the low-density liquid and high-density liquid phases is still missing.

What type of potential would be appropriate for describing the tetrahedrally bonded molecular liquids? Directional interactions are certainly an important ingredient in obtaining a quantitative prediction for network-forming liquids such as water. However, the models that are obtained from that approach are too complicated, being impossible to go beyond mean-field analysis. Isotropic models became the simplest framework to understand the physics of the liquid-liquid phase transition and liquid state anomalies. From the desire of constructing a simple two-body isotropic potential capable of describing the complicated behavior present in waterlike molecules, a number of models in which single component systems of particles interact via core-softened (CS) potentials²⁰ have been proposed. They possess a repulsive

^{a)}Electronic mail: oliveira@if.ufrgs.br

core that exhibits a region of softening where the slope changes dramatically. This region can be a shoulder or a ramp.^{21–36}

In the first case, the potential consists of a hard core, a square repulsive shoulder, and, in some cases, an attractive square well.^{21–31,34} In two dimensions, such potentials have density and diffusion anomalies and in some cases a second critical point.^{22,27–29} In three dimensions, these potentials do not have dynamic and thermodynamic anomalies but possess a second³⁰ and sometimes a third²⁵ critical point, accessible by simulations in the region predicted by the hypernetted chain integral equation.^{23,26,31}

In the second case, the interaction potential has two competing equilibrium distances, defined by a repulsive ramp.^{33–35} By including a global term for attraction, this model displays a liquid phase with a first-order line of liquid-gas transition ending in a critical point and a liquid-liquid phase transition ending in a second critical point.^{33,36}

Notwithstanding the progresses made by the models described above, a potential in which both the potential and the force are continuous functions and that exhibits all the thermodynamic and dynamic anomalies present in water is still missing. In this paper, we check if particles interacting with a core-softened potential similar to the one proposed by Cho *et al.*^{37,38} and Netz *et al.*³⁹ exhibit thermodynamic and dynamic anomalies similar to the ones present in water. Since the potential can have a variety of shapes, depending on its parameters, we study a soft ramp (with continuous force) with two scale distances. This type of potential gives a distribution function similar to the one expected for SPC/E water.⁴⁰ We check if the region in the pressure-temperature phase diagram of thermodynamic anomalies is inside the region of dynamic anomalies as in SPC/E water.¹⁰

The remainder of this paper goes as follows. In Sec. II the model is introduced; in Sec. III the phase diagram is obtained within the Rogers-Young, Percus-Yevick, and hypernetted chain integral equations. Results for the phase diagram and for the diffusion constant obtained from molecular-dynamics simulations are shown in Sec. IV. Conclusions about the relation between the locus of the density anomaly and the diffusion anomaly are presented in Sec. V.

II. THE MODEL

We consider a set of molecules of diameter σ interacting through a potential that consists of a combination of a Lennard-Jones potential of well depth ϵ plus a Gaussian well centered on radius $r=r_0$ with depth a and width c ,

$$U(r) = 4\epsilon \left[\left(\frac{\sigma}{r} \right)^{12} - \left(\frac{\sigma}{r} \right)^6 \right] + a\epsilon \exp \left[-\frac{1}{c^2} \left(\frac{r-r_0}{\sigma} \right)^2 \right]. \quad (1)$$

This potential can represent a whole family of two length scales intermolecular interactions, from a deep double-well potential^{37,39} to a repulsive shoulder,³³ depending on the choice of the values of a , r_0 , and c . Specific choices of these parameters lead to double-well potentials similar to the one studied by Cho *et al.*³⁷ The attractive

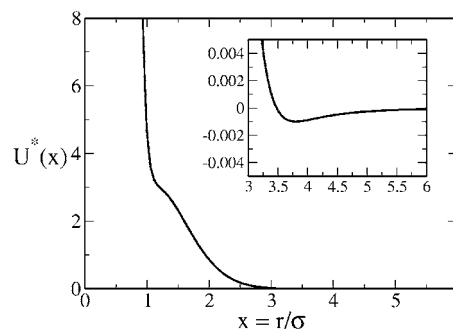


FIG. 1. Interaction potential Eq. (1) with parameters $a=5$, $r_0/\sigma=0.7$, and $c=1$, in reduced units. The inset shows a zoom in the very small attractive part of the potential.

double well brings both the liquid-gas phase transition and the anomalies to higher temperatures into the unstable region of the p - T phase diagram.³⁹

In order to circumvent this difficulty, here we investigate the thermodynamic and dynamic behaviors of particles interacting via a potential with a very small attractive region. We use Eq. (1) with $a=5$, $r_0/\sigma=0.7$, and $c=1$. This potential has two length scales within a repulsive ramp followed by a very small attractive well (Fig. 1).

In order to have an overview of the behavior of particles interacting with this potential, we use integral equations to estimate the thermodynamic properties in the phase diagram.

III. INTEGRAL EQUATIONS

One of the most successful theories for describing the structure of simple fluids are the integral equations.⁴¹ Among them, certainly the most famous is the Ornstein-Zernike (OZ) equation⁴² that, for pure isotropic fluids with density ρ , gives an exact relation between the direct correlation function, $c(r)$, and the total correlation function, $h(r)$, and it is given by

$$\gamma(r) = h(r) - c(r) = \rho \int h(\mathbf{r})c(|\mathbf{r} - \mathbf{r}'|)d\mathbf{r}', \quad (2)$$

where $h(r)=g(r)-1$ and where $g(r)$ is the pair distribution function. $g(r)$ is proportional to the probability to find a particle at a distance r when another particle is placed at the origin.

The Fourier transform of Eq. (2) is given by

$$\Gamma(k) = \frac{\rho C(k)^2}{1 - \rho C(k)}, \quad (3)$$

where $\Gamma(k)$ and $C(k)$ are the Fourier transforms of $\gamma(r)$ and $c(r)$, and the definition for the direct correlation function,

$$c(r) = h(r) - \ln\{g(r)\exp[\beta U(r)]\} + B(r), \quad (4)$$

was used. Here $\beta=1/k_B T$ and $B(r)$ is the sum of all bridge diagrams for the interparticle potential. Equation (3) together with Eq. (4) can be solved for a given interparticle potential. For obtaining $B(r)$ many approximations (*closure* relations) have been proposed^{43–49} along the years. Unfortunately, these approximations have the following thermodynamic in-

consistence: The pressure calculated via the *fluctuations* route,

$$\beta P_{\text{fluc.}} = \rho - 4\pi \int_0^\rho \rho' \int_0^\infty r^2 c(r, \rho') dr d\rho', \quad (5)$$

differs from the pressure calculated via the *virial* route,

$$\beta P_{\text{vir.}} = \rho - \frac{2\pi}{3} \rho^2 \beta \int_0^\infty r^3 \frac{dU(r)}{dr} g(r) dr. \quad (6)$$

Two of these closures have been widely used: the Percus-Yevick⁴³ (PY) where

$$B(r) = \ln[1 + \gamma(r)] - \gamma(r), \quad (7)$$

and the hypernetted chain⁴⁴ (HNC) that sets

$$B(r) = 0. \quad (8)$$

While HNC is appropriate for large interparticle distances, PY is more adequate for small ones. In order to avoid the inconsistencies present in the original integral equations, Rogers and Young⁵⁰ proposed a mix of the HNC and PY closures of the form

$$c(r) = \exp[-\beta U(r)] \left[1 + \frac{\exp[\gamma(r)f(r)] - 1}{f(r)} \right] - \gamma(r) - 1, \quad (9)$$

with the mixing function $f(r) = 1 - \exp[-\alpha r]$. Note that at $r=0$ Eq. (9) reduces to the PY approximation and for $r \rightarrow \infty$, Eq. (9) tends to the HNC approximation. The Rogers-Young (RY) approximation puts together PY and HNC closures with an adjustable parameter α . This parameter is determined by imposing that the pressure calculated using Eq. (5) gives the same result as using Eq. (6) (*global* consistency criterion). This method has the inconvenience of the integral in ρ' . Instead of calculating α by imposing that the pressure should be the same when calculated using Eqs. (5) and (6), one can obtain α by checking the consistency between the compressibilities χ_{fluc} and χ_{vir} , calculated by derivation of Eqs. (5) and (6), respectively,⁵¹ namely,

$$\frac{\beta}{\rho} \chi_{\text{fluc.}}^{-1} = 1 - 4\pi \rho \int_0^\infty r^2 c(r) dr \quad (10)$$

and

$$\frac{\beta}{\rho} \chi_{\text{vir.}}^{-1} = 1 - \frac{4\pi}{3} \rho \beta \int_0^\infty r^3 \frac{dU(r)}{dr} g(r) dr - \frac{2\pi}{3} \rho^2 \beta \int_0^\infty r^3 \frac{dU(r)}{dr} \frac{\partial g(\rho, r)}{\partial \rho} dr. \quad (11)$$

Others closures were proposed where one^{51,52} or more adjustable parameters^{53–55} are needed in order to guarantee the consistency. In this work, we use the RY approximation due its success in describing the structure of the systems whose particles interact by a purely repulsive pair potential.^{35,50,56,57}

A numerical iterative solution of the system formed by Eqs. (3) and (9) was performed using a fine grid with $M=4096$ points and a step size $\Delta x=0.0075$, from $x=r/\sigma$

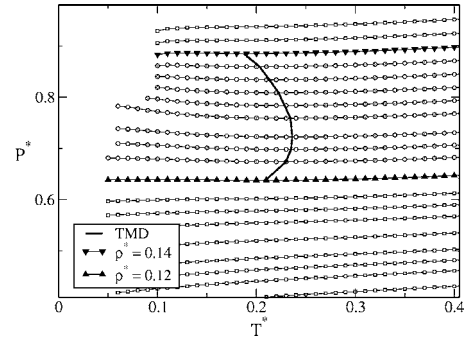


FIG. 2. Pressure-temperature phase diagram obtained by Rogers-Young integral equations. From bottom to top, the isochores $\rho=0.100, 0.103, 0.105, 0.107, 0.110, 0.113, 0.115, 0.117, 0.120, 0.123, 0.125, 0.127, 0.130, 0.132, 0.136, 0.138, 0.140, 0.142$, and 0.144 are shown. The solid line illustrates the TMD.

$=0.0075$ until $x=M\Delta x$. The tolerance for thermodynamic consistency was $1 - \chi_{\text{fluc.}}/\chi_{\text{vir.}} < 10^{-3}$. For the PY and HNC closures, the same M and Δx was used, in the same range. Pressure, temperature, and density are shown in dimensionless units,

$$T^* \equiv \frac{k_B T}{\epsilon}, \quad (12)$$

$$\rho^* \equiv \rho \sigma^3, \quad (13)$$

$$P^* \equiv \frac{P \sigma^3}{\epsilon}. \quad (14)$$

The main features of the phase diagram obtained by RY closure are illustrated in Fig. 2. This p - T phase diagram shows that the isochores with $0.120 \leq \rho^* \leq 0.140$ have a minimum which means that $(\partial P / \partial T)_\rho = 0$. From this follows $(\partial \rho / \partial T)_P = 0$, which implies a density anomaly. The line of minima for the different isochores forms the temperatures of maximum density (TMD) shown in Fig. 2 by a solid line.

The presence of a possible critical point between two liquid phases may be suggested by the crossing of the analytic continuation of isochores $\rho^*=0.134, 0.136, 0.138, 0.140, 0.142$, and 0.144 , in the region below $T^* < 0.05$. In this region the integral equations numerical solutions do not

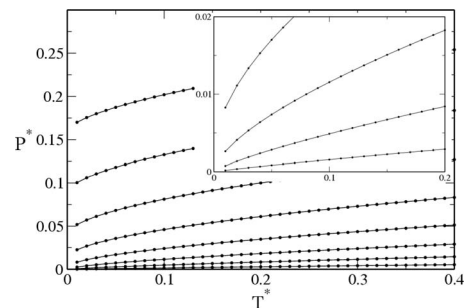


FIG. 3. Phase diagram in Rogers-Young integral equations. The low isochores $\rho=0.01, 0.02, 0.03, 0.04, 0.05, 0.06, 0.07$, and 0.08 , from bottom to top, are shown. The inset shows the isochores for $\rho^*=0.01, 0.02, 0.03$, and 0.04 . For $\rho^* \leq 0.03$, the isochores are converging to a point at the supercooled region—the liquid-gas phase transition.

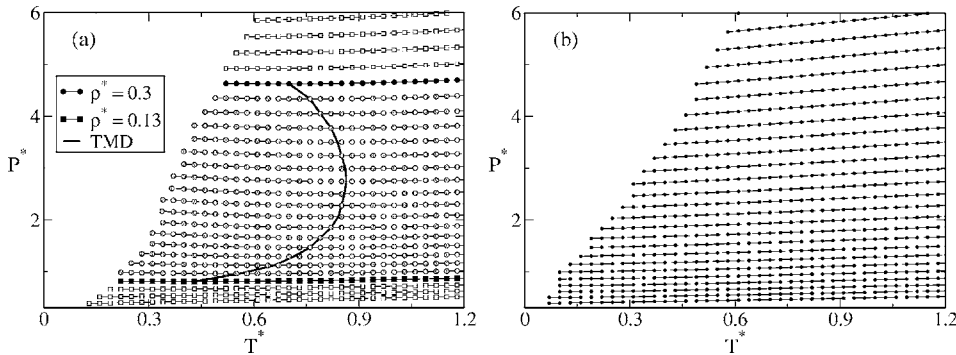


FIG. 4. p - T phase diagram obtained by PY (a) and HNC (b) integral equations. From bottom to top, the twenty five isochores illustrated are $\rho=0.10, 0.11, 0.12, \dots, 0.33$, and 0.34 . in both figures. The solid line in (a) illustrates the TMD line.

converge and the thermodynamic equilibrium is not achieved for the molecular-dynamics (MD) simulations.

Figure 3 shows that the very low isochores at $\rho^* \leq 0.03$ are converging to a point in the supercooled region, indicating a liquid-gas critical point, as can be seen from the inset.

When analyzing the model Eq. (1) with the PY approximation, density anomaly was found between $0.13 < \rho^* < 0.3$ in a region of temperatures from $0.4 < T^* < 0.86$, as can be seen from Fig. 4(a). No density anomaly was found when the model Eq. (1) was analyzed with HNC [Fig. 4(b)].

IV. THE MOLECULAR DYNAMICS

We also performed molecular-dynamics simulations in the canonical ensemble using 500 particles in a cubic box with periodic boundary conditions, interacting with the intermolecular potential described above. The chosen parameters were $a=5.0$, $r_0/\sigma=0.7$, and $c=1.0$. The cutoff radius was set to 3.5 length units. Using reduced units defined as T^* and ρ^* , a broad range of temperatures ($0.10 \leq T^* \leq 0.45$) and densities ($0.05 \leq \rho^* \leq 1.00$) was chosen, in order to explore the phase diagram. Thermodynamic and dynamic properties were calculated over 2 500 000 steps long simulations, previously equilibrated over 500 000 steps. In the lower temperature systems, additional simulations were carried out with equilibration over 2 000 000 steps, followed by a 6 000 000 simulation run. The time step was 0.001 in reduced units. The thermodynamical stability of the system was checked by analyzing the dependence of pressure on density and also by visual analysis of the final structure, searching for cavitation.

Figure 5 shows the p - T phase diagram obtained by molecular dynamics. The isochores have minima that define the temperature of maximum density. The TMD line encloses the region of density (and entropy) anomaly. The comparison between the RY and MD results shows that the TMD line starts at lower densities in the MD simulations than that in RY integral equations. Above $\rho^*=0.144$ both theories agree that no density anomaly happens. The RY pressures for each isochore are slightly underestimated when compared with simulations, but the overall agreement between the predictions of this closure and the simulation results is very good. On the other side, the PY approximation predicts density anomaly, but in a region completely different than that of MD. The HNC closure does not show a TMD line, as we have discussed before.

The MD simulations also indicate the possibility of a liquid-liquid critical point by the crossing of the analytic continuation of isochores $\rho^*=0.134, 0.136, 0.138, 0.140, 0.142$, and 0.144 ; the same behavior was seen by the RY closure, and missing by PY and HNC.

We also study the mobility associated with the potential described in Eq. (1). The diffusion is calculated using the the mean-square displacement averaged over different initial times,

$$\langle \Delta r(t)^2 \rangle = \langle [r(t_0 + t) - r(t_0)]^2 \rangle. \quad (15)$$

Then the diffusion coefficient is obtained from the relation

$$D = \lim_{t \rightarrow \infty} \langle \Delta r(t)^2 \rangle / 6t. \quad (16)$$

Figure 6 shows the behavior of the translational diffusion coefficient,

$$D^* \equiv \frac{D(m/\epsilon)^{1/2}}{\sigma}, \quad (17)$$

as a function of ρ^* . At low temperatures, the behavior is similar to the behavior found¹⁰ in SPC/E supercooled water. The diffusivity increases as the density is lowered, reaches a maximum at $\rho_{D\max}$ (and $P_{D\max}$) and decreases until it reaches a minimum at $\rho_{D\min}$ (and $P_{D\min}$).

The region in the p - T plane where there is an anomalous behavior in the diffusion is bounded by $(T_{D\min}, P_{D\min})$ and $(T_{D\max}, P_{D\max})$ and their location is shown in Fig. 5. The

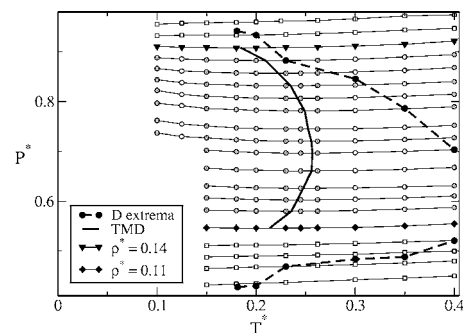


FIG. 5. Pressure-temperature phase diagram obtained by molecular-dynamics simulation. From bottom to top, the same isochores illustrated in RY phase diagram, $\rho=0.100, 0.103, 0.105, 0.107, 0.110, 0.113, 0.115, 0.117, 0.120, 0.123, 0.125, 0.127, 0.130, 0.132, 0.134, 0.136, 0.138, 0.140, 0.142$, and 0.144 are shown. The solid line illustrates the TMD and the dashed line shows the boundary of the diffusivity extrema.

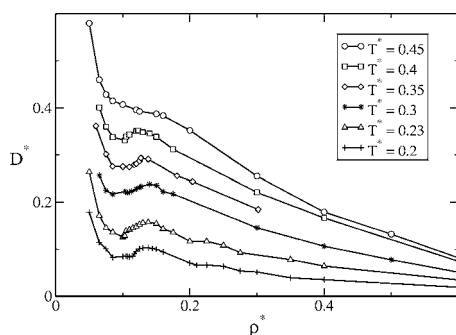


FIG. 6. Diffusion coefficient as a function of density for some studied temperatures. The units are defined in the text.

region of diffusion anomalies ($T_{D\max}, P_{D\max}$) and ($T_{D\min}, P_{D\min}$) lies outside the region of density anomalies such as in SPC/E water.¹⁰

V. CONCLUSIONS

We have studied the thermodynamic properties of fluids interacting via a three-dimensional continuous core-softened potential with a continuous force, using several integral equations closures, RY, PY, and HNC, as well as molecular-dynamics simulations. The continuity of the force is similar that one expects for realistic systems. We studied the density anomaly and anomalies in the translational diffusion. Both RY integral equations and molecular-dynamics results show that the density can behave anomalously at a certain range of pressures and temperatures. The agreement between these two theories is very good, confirming the RY integral equations as a powerful tool for investigations of interatomic repulsive pair potentials. The PY approximation emphasizes the short-ranged interactions and indeed predicts density anomaly, but the width of the anomaly region is strongly overestimated if compared with MD simulations. No density anomaly was found employing the HNC closure, because this approach is better suited for systems with long-ranged interactions.

Both MD and RY theories suggest the possibility of a second critical point, between two liquid phases, by the crossing of the analytic continuation of the isochores where $0.134 \leq \rho^* \leq 0.144$ for $T^* < 0.05$. However, the actual calculations or simulations in this region were not possible, either by failure in the integral equations convergence or because the equilibrium was not reached.

The translational diffusion shows a maximum and a minimum in the pressure-temperature phase diagram. The region in the p - T plane of density anomaly is located inside the region of the anomalous diffusion.

The studied continuous core-softened potential, despite not having long-ranged or H-bond-like directional interactions, exhibit thermodynamic and dynamic anomalies similar to the ones observed in SPC/E water.¹⁰

ACKNOWLEDGMENTS

We thank Anatol Malijevsky for having introduced us to the computational methods to the integral equations, Gian-

carlo Franzese for fruitful discussions about the potential, and the Brazilian science agencies CNPq, FINEP, and Fapergs for financial support.

- ¹R. Waller, *Essays of Natural Experiments* (Johnson Reprint, New York, 1964).
- ²F. X. Prielmeier, E. W. Lang, R. J. Speedy, and H.-D. Lüdemann, *Phys. Rev. Lett.* **59**, 1128 (1987).
- ³F. X. Prielmeier, E. W. Lang, R. J. Speedy, and H.-D. Lüdemann, *Ber. Bunsenges. Phys. Chem.* **92**, 1111 (1988).
- ⁴L. Haar, J. S. Gallagher, and G. S. Kell, *NBS/NRC Steam Tables. Thermodynamic and Transport Properties and Computer Programs for Vapor and Liquid States of Water in SI Units* (Hemisphere, Washington D.C., 1984), pp. 271–276.
- ⁵F. W. Starr, F. Sciortino, and H. E. Stanley, *Phys. Rev. E* **60**, 6757 (1999); F. W. Starr, S. T. Harrington, F. Sciortino, and H. E. Stanley, *Phys. Rev. Lett.* **82**, 3629 (1999).
- ⁶P. Gallo, F. Sciortino, P. Tartaglia, and S.-H. Chen, *Phys. Rev. Lett.* **76**, 2730 (1996); F. Sciortino, P. Gallo, P. Tartaglia, and S.-H. Chen, *Phys. Rev. E* **54**, 6331 (1996); S.-H. Chen, F. Sciortino, and P. Tartaglia, *ibid.* **56**, 4231 (1997); F. Sciortino, L. Fabbian, S.-H. Chen, and P. Tartaglia, *ibid.* **56**, 5397 (1997).
- ⁷S. Harrington, P. H. Poole, F. Sciortino, and H. E. Stanley, *J. Chem. Phys.* **107**, 7443 (1997).
- ⁸F. Sciortino, A. Geiger, and H. E. Stanley, *Nature (London)* **354**, 218 (1991); *J. Chem. Phys.* **96**, 3857 (1992).
- ⁹J. R. Errington and P. G. Debenedetti, *Nature (London)* **409**, 318 (2001).
- ¹⁰P. A. Netz, F. W. Starr, H. E. Stanley, and M. C. Barbosa, *J. Chem. Phys.* **115**, 344 (2001).
- ¹¹P. A. Netz, F. W. Starr, M. C. Barbosa, and H. E. Stanley, *Physica A* **314**, 470 (2002).
- ¹²H. E. Stanley, M. C. Barbosa, S. Mossa, P. A. Netz, F. Sciortino, F. W. Starr, and M. Yamada, *Physica A* **315**, 281 (2002).
- ¹³P. A. Netz, F. W. Starr, M. C. Barbosa, and H. E. Stanley, *J. Mol. Liq.* **101**, 159 (2002).
- ¹⁴P. H. Poole, F. Sciortino, U. Essmann, and H. E. Stanley, *Nature (London)* **360**, 324 (1992); *Phys. Rev. E* **48**, 3799 (1993); F. Sciortino, P. H. Poole, U. Essmann, and H. E. Stanley, *ibid.* **55**, 727 (1997); S. Harrington, R. Zhang, P. H. Poole, F. Sciortino, and H. E. Stanley, *Phys. Rev. Lett.* **78**, 2409 (1997).
- ¹⁵Y. Katayama, T. Mizutani, W. Utsumi, O. Shimomura, M. Yamakata, and K. Funakoshi, *Nature (London)* **403**, 170 (2000).
- ¹⁶G. Monaco, S. Falconi, W. A. Crichton, and M. Mezouar, *Phys. Rev. Lett.* **90**, 255701 (2003).
- ¹⁷D. J. Lacks, *Phys. Rev. Lett.* **84**, 4629 (2000).
- ¹⁸P. T. Cummings and G. Stell, *Mol. Phys.* **43**, 1267 (1981).
- ¹⁹M. Togaya, *Phys. Rev. Lett.* **79**, 2474 (1997).
- ²⁰For a recent review, see P. Debenedetti, *J. Phys.: Condens. Matter* **15**, R1669 (2003).
- ²¹M. R. Sadr-Lahijany, A. Scala, S. V. Buldyrev, and H. E. Stanley, *Phys. Rev. Lett.* **81**, 4895 (1998); *Phys. Rev. E* **60**, 6714 (1999).
- ²²A. Scala, M. R. Sadr-Lahijany, N. Giovambattista, S. V. Buldyrev, and H. E. Stanley, *J. Stat. Phys.* **100**, 97 (2000); *Phys. Rev. E* **63**, 041202 (2001).
- ²³G. Franzese, G. Malescio, A. Skibinsky, S. V. Buldyrev, and H. E. Stanley, *Nature (London)* **409**, 692 (2001).
- ²⁴S. V. Buldyrev, G. Franzese, N. Giovambattista, G. Malescio, M. R. Sadr-Lahijany, A. Scala, A. Skibinsky, and H. E. Stanley, *Physica A* **304**, 23 (2002).
- ²⁵S. V. Buldyrev and H. E. Stanley, *Physica A* **330**, 124 (2003).
- ²⁶G. Franzese, G. Malescio, A. Skibinsky, S. V. Buldyrev, and H. E. Stanley, *Phys. Rev. E* **66**, 051206 (2002).
- ²⁷A. Balladares and M. C. Barbosa, *J. Phys.: Condens. Matter* **16**, 8811 (2004).
- ²⁸A. B. de Oliveira and M. C. Barbosa, *J. Phys.: Condens. Matter* **17**, 399 (2005).
- ²⁹V. B. Henriques and M. C. Barbosa, *Phys. Rev. E* **71**, 031504 (2005); V. B. Henriques, N. Guisconi, M. A. Barbosa, M. Thielo, and M. C. Barbosa, *Mol. Phys.* **103**, 3001 (2005).
- ³⁰A. Skibinsky, S. V. Buldyrev, G. Franzese, G. Malescio, and H. E. Stanley, *Phys. Rev. E* **69**, 061206 (2004).
- ³¹G. Malescio, G. Franzese, A. Skibinsky, S. V. Buldyrev, and H. E. Stanley, *Phys. Rev. E* **71**, 061504 (2005).

- ³²P. C. Hemmer, and G. Stell, Phys. Rev. Lett. **24**, 1284 (1970); G. Stell and P. C. Hemmer, J. Chem. Phys. **56**, 4274 (1972); J. M. Kincaid, G. Stell, and C. K. Hall, *ibid.* **65**, 2161 (1976); J. M. Kincaid, G. Stell, and E. Goldmark, *ibid.* **65**, 2172 (1976); C. K. Hall and G. Stell, Phys. Rev. A **7**, 1679 (1973); E. Velasco, L. Medeiros, G. Navascués, P. C. Hemmer, and G. Stell, Phys. Rev. Lett. **85**, 122 (2000); P. C. Hemmer, E. Velasco, L. Mederos, G. Navascués, and G. Stell, J. Chem. Phys. **114**, 2268 (2001).
- ³³E. A. Jagla, Phys. Rev. E **58**, 1478 (1998); J. Chem. Phys. **110**, 451 (1999); **111**, 8980 (1999); Phys. Rev. E **63**, 061501 (2001); **63**, 061509 (2001).
- ³⁴N. B. Wilding and J. E. Magee, Phys. Rev. E **66**, 031509 (2002).
- ³⁵P. Kumar, S. V. Buldyrev, F. Sciortino, E. Zaccarelli, and H. E. Stanley, Phys. Rev. E **72**, 021501 (2005).
- ³⁶L. Xu, P. Kumar, S. V. Buldyrev, S.-H. Chen, P. H. Poole, F. Sciortino, and H. E. Stanley, Proc. Natl. Acad. Sci. U.S.A. **102**, 16558 (2005).
- ³⁷C. H. Cho, S. Singh, and G. W. Robinson, Phys. Rev. Lett. **76**, 1651 (1996); Faraday Discuss. **103**, 19 (1996); J. Chem. Phys. **107**, 7979 (1997).
- ³⁸C. H. Cho, S. Singh, and G. W. Robinson, Phys. Rev. Lett. **79**, 180 (1997).
- ³⁹P. A. Netz, J. Fernando Raymundi, A. S. Camera, and M. C. Barbosa, Physica A **342**, 48 (2004).
- ⁴⁰T. Head-Gordon and F. H. Stillinger, J. Chem. Phys. **98**, 3313 (1993).
- ⁴¹J. P. Hansen and I. R. McDonald, *Theory of Simple Liquids*, 2nd ed. (London Academic, London, 1986).
- ⁴²L. S. Ornstein and F. Zernike, Proc. R. Acad. Sci. Amsterdam **17**, 793 (1914).
- ⁴³J. K. Percus and G. J. Yevick, Phys. Rev. **110**, 1 (1958).
- ⁴⁴J. M. J. van Leeuwen, J. Groenvelt, and J. De Boer, Physica (Amsterdam) **25**, 792 (1959).
- ⁴⁵J. L. Lebowitz and J. K. Percus, Phys. Rev. **144**, 251 (1966).
- ⁴⁶L. Verlet, Mol. Phys. **41**, 183 (1980).
- ⁴⁷G. A. Martynov and G. N. Sarkisov, Mol. Phys. **49**, 1495 (1983).
- ⁴⁸P. Ballone, G. Pastore, G. Galli, and D. Gazzillo, Mol. Phys. **59**, 275 (1986).
- ⁴⁹L. L. Lee, J. Chem. Phys. **97**, 8606 (1992).
- ⁵⁰F. J. Rogers and D. A. Young, Phys. Rev. A **30**, 999 (1984).
- ⁵¹G. Zerah and J.-P. Hansen, J. Chem. Phys. **84**, 2336 (1986).
- ⁵²J. M. Bomont and J. L. Bretonnet, Mol. Phys. **101**, 3249 (2003).
- ⁵³D. S. Hall and W. R. Conkie, Mol. Phys. **40**, 907 (1980).
- ⁵⁴A. Malijevsky and S. Labik, Mol. Phys. **60**, 663 (1987).
- ⁵⁵L. L. Lee and A. Malijevsky, J. Chem. Phys. **114**, 7109 (2001).
- ⁵⁶A. Lang, G. Kahl, C. N. Likos, H. Lowen, and M. Watzlawek, J. Phys.: Condens. Matter **11**, 10143 (1999).
- ⁵⁷C. N. Likos, H. Lowen, M. Watzlawek, B. Abbas, O. Jucknischke, J. Allgaier, and D. Richter, Phys. Rev. Lett. **80**, 4450 (1998).